

Synthesis of Output-Feedback Controllers for Mixed Traffic Systems in Presence of Disturbances and Uncertainties

Shima Sadat Mousavi[†], Somayeh Bahrami[‡], and Anastasios Kouvelas[†]

Abstract—In this paper, we study mixed traffic systems that move along a single-lane ring-road or open-road. The traffic flow forms a platoon, which includes a number of heterogeneous human-driven vehicles (HDVs) together with only one connected and automated vehicle (CAV) that receives information from several neighbors. The dynamics of HDVs are assumed to follow the optimal velocity model (OVM), and the acceleration of the single CAV is directly controlled by a dynamical output-feedback controller. The ultimate goal of this work is to present a robust control strategy that can smoothen the traffic flow in the presence of undesired disturbances (e.g. abrupt deceleration) and parametric uncertainties. A prerequisite for synthesizing a dynamical output controller is the stabilizability and detectability of the underlying system. Accordingly, a theoretical analysis is presented first to prove the stabilizability and detectability of the mixed traffic flow system. Then, two H_∞ control strategies, with and without considering uncertainties in the system dynamics, are designed. The efficiency of the two control methods is subsequently illustrated through numerical simulations, and various experimental results are presented to demonstrate the effectiveness of the proposed controller to mitigate disturbance amplification and achieve platoon stability.

I. INTRODUCTION

In recent decades, thanks to developments in automation, such as the emergence of automated vehicles or automated infrastructures, a tremendous revolution has occurred in transportation systems. The transition phase from using only human-driven vehicles (HDVs) to fully connected and automated vehicles (CAVs) results in new challenges and creates a strong motivation to study the mixed traffic systems, that include both HDVs and CAVs (e.g., see [1], [2] and the references therein). In this direction, new opportunities arise to utilize the potential abilities of CAVs to control a transportation network, manage congestion, and promote the efficiency and safety of traffic systems.

More traditional methodologies for controlling traffic flow employ controllers and actuators at fixed locations, among which variable speed limits (VSLs) and ramp metering (RMs) can be mentioned [3]. However, the installation of these actuators is not cost-effective and reduces the flexibility of the control system. On the other hand, the advent of CAVs as mobile actuators—so-called Lagrangian actuators—paves the way for applying traffic flow control in a more effective and flexible manner. For instance, if all the involved vehicles are CAVs, efficient control strategies, such as adaptive cruise control (ACC) and cooperative adaptive cruise control (CACC), can be employed and lead to a desirable system performance

[4], [5], [6], [7]. Nevertheless, in a mixed traffic system, where the penetration rate of CAVs is less than one, new challenges are introduced that require further theoretical and experimental analyses.

In this direction, we consider a mixed traffic system, including one CAV and numerous HDVs, for the two common scenarios of a ring-road and an open-road and reveal how the single CAV is capable of controlling the entire network. In the following, we first present a review of some relevant works in the literature, and subsequently, we discuss the main contributions of this work.

A. Literature Review

There are a few experimental studies that verify the emergence of stop-and-go waves in traffic flow systems. For instance, in the study in [8], the outcome of a practical experiment on a single-lane ring-road demonstrated that a platoon consisting only of HDVs has the potential to initiate stop-and-go waves. These waves that travel upstream along the road make a uniform flow unstable and create a so-called *phantom traffic jam*. This phenomenon of instability has been studied in the literature from macroscopic [9], cellular automaton [10], and microscopic [11] point of view. The emerging nonlinear waves can be amplified by some effects such as stochastic behaviour of human drivers, lane changing, road characteristics, and ramps, to name a few. In [12], a field experiment was conducted to show that utilizing a single CAV in a platoon on a circular roadway can dissipate the undesired waves. Moreover, in [13], through some theoretical analysis, the capability of a single CAV to control the traffic flow on a ring-road was investigated.

In fact, since the platoon is connected, and neighboring vehicles can interact, a sparse number of CAVs—that act as mobile actuators—can influence the whole network and stabilize the traffic system. The notions of string and ring stability have been employed here for the stability analysis of interconnected vehicles on a string and on a ring roadway, respectively [14], [15], [16]. In the same direction, and for mixed traffic systems, the string stability of a mixed platoon of infinite length has been analyzed in [17]. Furthermore, in [18], a linear stability condition has been stated in terms of the penetration rate and spatial distribution of CAVs.

In order to dissipate stop-and-go waves in a mixed traffic system, an appropriate control strategy can be provided that is applied to the CAVs as the controllers. To establish a theoretical analysis for these systems, we should first derive a mathematical model that represents the dynamical behaviour of HDVs. In this direction, there are different car-following models, among which the optimal-velocity-follow-the-leader

[†]The authors are with the Institute for Transport Planning and Systems, ETH Zurich, Switzerland, {shimaossadat.mousavi, anastasios.kouvelas}@ivt.baug.ethz.ch

[‡]The author is with the Department of Electrical Engineering, Razi University, Kermanshah, Iran, s.bahrami@razi.ac.ir

(OV-FTL) model [11] and the intelligent driver model (IDM) [19] can be indicated. These models are nonlinear in principle, but most of studies in the field of mixed traffic systems utilize a linearized version of the nonlinear dynamics around the equilibrium flow (see e.g., [20], [21], [16], [22], [23]).

A fundamental network property that should be checked before designing a controller is its controllability or stabilizability [24], [25], [26]. If a linear system is controllable, then a control signal can be designed to steer the system from any initial state to any final state within finite time. A weaker condition that is necessary for the existence of a controller is the stabilizability of a system. A linear system is stabilizable if with a suitable choice of control signals, all the states remain bounded or converge to constant values [27]. Recently, some works in the literature have focused on providing a rigorous controllability and stabilizability analysis for ring-road mixed traffic systems with one single CAV.

In [13], [22], it is assumed that all HDVs in the platoon are homogeneous, which is a strong assumption for practical scenarios. In fact, the problem where heterogeneity of HDVs is considered is closer to reality, but theoretically more challenging. In [28], [23], a controllability analysis for mixed traffic systems, including one CAV and a number of heterogeneous HDVs, is provided. It is stated that under a restrictive condition on parameters of the dynamic model, all nonzero eigenvalues of the system are controllable; while there exists only one uncontrollable eigenvalue at origin. More recently, in [29], by considering the similar condition on the parameters of the system, the controllability of a so-called “1+n” mixed platoon, forming a string at a signalized intersection, is provided. Moreover, in [30], by defining a new notion of leading cruise control, the controllability of a platoon along a string is analyzed. None of these works provide the controllability analysis of a mixed platoon in the most general case and without assuming any constraint on the system parameters.

There are numerous works in the literature, proposing various control strategies to stabilize a mixed platoon on an open-road or a ring-road [31], [32], [13], [33], [12], [34], [35]. However, in most of these works, the communication topology of the network which represents the capability of the CAV to receive information from its neighboring vehicles has been neglected [31], [36], [20], [37], [35], and it has been assumed that it can be connected to any vehicle in the platoon. More recently, in [28], the issue of limited communication has been considered, and a *structured* optimal control has been proposed, which is in general computationally intractable [38] and results in a sub-optimal solution. In addition, the HDVs usually do not follow deterministic dynamic models, and there exists uncertainties in the model parameters of HDVs, that can affect the efficiency of the control strategies. Accordingly, it is needed to provide robust control methods that dissipate the perturbations of the traffic flow in the presence of system uncertainties (see e.g., [39], [40], [41]).

B. Contributions

In this paper, we consider a mixed traffic system with one CAV and numerous heterogeneous HDVs. The mixed

platoon is studied in two cases of a ring-road and an open-road. The traffic system is modeled at a microscopic scale, and the dynamics of HDVs are represented by the optimal velocity model. Furthermore, the acceleration of the CAV is directly controlled. For this system, we first establish a stabilizability analysis for the two cases of a ring-road and an open-road. Moreover, since the goal is to synthesize an output-feedback controller, the detectability analysis of the system is also necessary, which is presented subsequently. As a real-world scenario, we also consider the limited communication capability of the CAV in this work. In order to deal with the topological communication constraints, we propose an output-feedback controller that employs the information of a sparse set of vehicles in the control signal design. Our proposed method offers a robust H_∞ controller, that not only increase the efficiency of the CAV, but it also dampens the disturbances appearing as nonlinear waves and improves the performance in the behavior of the entire traffic network.

In summary, the main contributions of this work are listed as follows:

- We analyze the controllability and observability of a mixed traffic system with one CAV and numerous heterogeneous HDVs for both common scenarios of a ring-road and an open-road in the most general case. In fact, unlike the existing works in the literature, such as [23], that investigates the stabilizability under restrictive parameter constraints, we prove that, for any value of system parameters, the mixed platoon is stabilizable. This analysis verifies the ability of the single CAV to make the states of all HDVs converge to desired values. Further, since we aim to synthesize a dynamic output controller that can utilize the states of only a subset of HDVs, we prove in this work that the mixed traffic system is also detectable.
- In order to dampen the undesired perturbations occurring in a mixed traffic flow where there is no uncertainties in the system parameters, we propose a solution based on synthesizing an H_∞ output dynamic feedback controller. This controller also tackles the issue of the CAV’s communication constraints. To the best of our knowledge, this is the first time in the literature that an output dynamic controller is utilized for the control of a mixed platoon. Unlike some existing control strategies, e.g., [7], [42], that aim to increase the local efficiency around the CAVs, our method offers a controller that improves the performance in the behavior of the entire traffic network. More importantly, as we consider a higher degree of freedom in designing the control strategy, our proposed control method leads to a global optimal solution, while the structural control method in [23] results is a sub-optimal one.
- As the next and the more practical scenario, we consider the model mismatch and parametric uncertainties in the dynamics of HDVs and provide a robust control strategy that can smoothen the traffic flow in the presence of disturbances and uncertainties.

C. Outline

The rest of this paper is organized as follow. In Section II, the model of a mixed traffic system is presented, and the main problems of this work are formulated. Section III discusses the stabilizability and detectability of a mixed platoon with a single CAV for both ring-road and open-road setups. In section IV, we propose an output dynamic controller for a mixed traffic flow that has no uncertainty in the system parameters. Section V establishes a control strategy that smoothen the traffic flow in the presence of uncertainties. In Section VI, numerical validations of the results as well as a numerical comparison with some of existing works in the literature are provided. Finally, Section VII concludes the paper.

II. PRELIMINARIES

In this section, we first present a dynamic model for a mixed traffic system on a single-lane ring-road, and then we formulate the problem.

We denote the set of real and complex numbers by \mathbb{R} and \mathbb{C} , respectively. For $a \in \mathbb{C}$, $\text{Re}(a)$ represents its real part. We denote the transpose of matrix M by M^T . Also, $\det(M)$ represents its determinant. For a vector space \mathcal{V} , $\dim(\mathcal{V})$ indicates its dimension. The identity matrix is denoted by I , and its j -th column is designated by e_j . Also, $0_{n \times m}$ represents an $n \times m$ zero matrix. We also show by 0 a zero matrix of an appropriate dimension. For $\alpha_1, \dots, \alpha_n \in \mathbb{R}$, $A = \text{diag}(\alpha_1, \dots, \alpha_n)$ is an $n \times n$ diagonal matrix whose diagonal elements are $\alpha_1, \dots, \alpha_n$. For a matrix $M \in \mathbb{R}^{n \times n}$, where $M = M^T$, $M \succ 0$ (resp., $M \succeq 0$) implies that M is a positive definite (resp., positive semi-definite) matrix. $\|\cdot\|$ denotes the Euclidean norm of vectors and the induced norm of matrices. Also, $\|\cdot\|_{\mathcal{F}}$ denotes Frobenius norm of matrices.

Fact 1: [43] For any matrix $A \in \mathbb{R}^{n \times n}$, we have $\|A\| < \|A\|_{\mathcal{F}}$, where $\|A\|_{\mathcal{F}} = (\sum_{i=1}^n \sum_{j=1}^n a_{ij}^2)^{\frac{1}{2}}$.

Fact 2: [43] For any matrix $A \in \mathbb{R}^{n \times n}$, $\|A\| \leq 1$ if and only if $A^T A \preceq I$.

A. Modeling a Mixed Traffic System

We study a mixed traffic system that is a network of n vehicles, including one CAV and $n - 1$ HDVs. We consider two cases of a single-lane ring-road and a single-lane open-road with length D . In Fig. 1(a), a schematic diagram of this network is illustrated, where the red car denotes the CAV, indexed with 1, and all others are HDVs. The position and velocity of vehicle i are denoted by p_i and v_i , respectively. We define as $s_i = p_{i-1} - p_i$ the back-to-back distance of the i -th vehicle from the $i - 1$ -th vehicle.

There are different models in the literature to represent the car-following dynamics of human-driven vehicles (see e.g., [19], [21], [11]). For instance, the optimal velocity model (OVM) [11] can be described as:

$$\begin{aligned} \dot{s}_i(t) &= v_{i-1}(t) - v_i(t) \\ \dot{v}_i(t) &= H_i(v_i(t), s_i(t), \dot{s}_i(t)), \end{aligned} \quad (1)$$

where $H_i(\cdot)$ is the acceleration of vehicle i , that is a nonlinear function of its velocity v_i , the spacing s_i , and the relative velocity \dot{s}_i . Note that unlike most of the works in literature

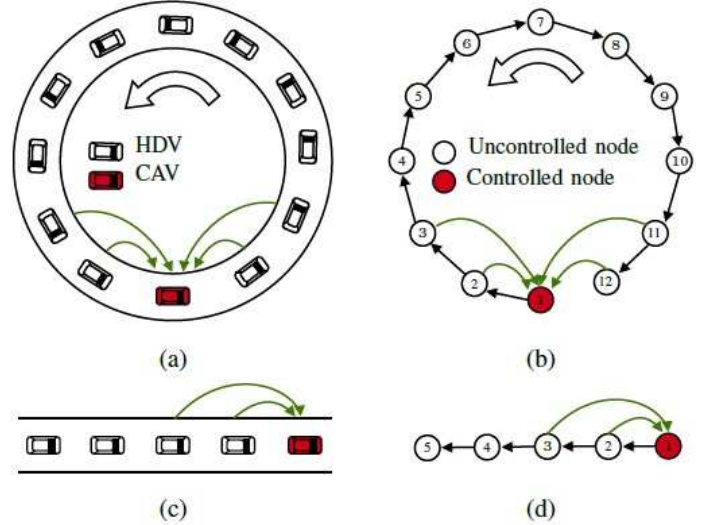


Fig. 1. (a)–(b) Schematic of a mixed traffic system on a ring-road and the corresponding graph; (c)–(d) Schematic of a mixed traffic system on an open-road and the corresponding graph.

(e.g., [13], [31], [2]), in this paper, HDVs are assumed to be heterogeneous, and thus, the dynamics of each vehicle i is described by a distinct nonlinear function $H_i(\cdot)$. One can see that at the equilibrium point of dynamics (1), all vehicles have the same velocity v^* . Moreover, since we have $\dot{v}^* = 0$, the spacing s_i^* is computed by $0 = H_i(v^*, s_i^*, 0)$. Now, let us define the state error $x_i^T = [\bar{s}_i \ \bar{v}_i] = [s_i - s_i^* \ v_i - v^*]$. Then, by linearization of (1) around the equilibrium point $[s_i^* \ v^*]^T$, for $i = 2, \dots, n$, one can derive a linear time-invariant (LTI) model for the i -th HDV as:

$$\begin{aligned} \dot{\bar{s}}_i(t) &= \bar{v}_{i-1}(t) - \bar{v}_i(t) \\ \dot{\bar{v}}_i(t) &= \beta_{i1} \bar{s}_i(t) - \beta_{i2} \bar{v}_i(t) + \beta_{i3} \bar{v}_{i-1}, \end{aligned}$$

where

$$\beta_{i1} = \frac{\partial H_i}{\partial s_i}, \quad \beta_{i2} = \frac{\partial H_i}{\partial \dot{s}_i} - \frac{\partial H_i}{\partial v_i}, \quad \beta_{i3} = \frac{\partial H_i}{\partial \dot{s}_i},$$

computed at the equilibrium point. Due to some physical constraints imposed by the behavior of HDVs in practice [13], one should consider

$$\beta_{i1} > 0, \quad \beta_{i2} > 0, \quad \beta_{i3} > 0. \quad (2)$$

Now, for the dynamics of the single CAV, we consider two cases of a ring-road and an open-road: 1) Corresponding to the case of a ring-road, the dynamics of the single CAV whose acceleration can be directly controlled are given by:

$$\begin{aligned} \dot{\bar{s}}_1(t) &= \bar{v}_n(t) - \bar{v}_1(t) \\ \dot{\bar{v}}_1(t) &= u(t) \end{aligned}, \quad (3)$$

where $u(t) \in \mathbb{R}$ is the control signal. 2) In the case of an open road, we have:

$$\begin{aligned} \dot{\bar{s}}_1(t) &= u_1(t) - \bar{v}_1(t) \\ \dot{\bar{v}}_1(t) &= u_2(t) \end{aligned}, \quad (4)$$

where $u_1(t), u_2(t) \in \mathbb{R}$ are two external inputs, and $u(t) = [u_1 \ u_2]^T \in \mathbb{R}^2$. In fact, in the case of an open-road, both

acceleration and velocity of the CAV are directed by external inputs.

Now, by defining the aggregated vector of states of all vehicles as $x = [x_1^T \ x_2^T \ \dots \ x_n^T]^T \in \mathbb{R}^{2n}$, one can derive the following LTI dynamics for the overall system:

$$\dot{x}(t) = Ax(t) + Bu(t), \quad (5)$$

$$A = \begin{bmatrix} J_1 & 0 & \dots & \dots & 0 & J_2 \\ A_{21} & A_{22} & 0 & \dots & \dots & 0 \\ 0 & A_{31} & A_{32} & 0 & \dots & 0 \\ \vdots & \ddots & \ddots & \ddots & \ddots & \vdots \\ 0 & \dots & \dots & 0 & A_{n1} & A_{n2} \end{bmatrix}, \quad B = \begin{bmatrix} B_1 \\ B_2 \\ B_2 \\ \vdots \\ B_2 \end{bmatrix}, \quad (6)$$

with $J_1 = \begin{bmatrix} 0 & -1 \\ 0 & 0 \end{bmatrix}$, and for $i = 2, \dots, n$, we have:

$$A_{i1} = \begin{bmatrix} 0 & 1 \\ 0 & \beta_{i3} \end{bmatrix}, \quad A_{i2} = \begin{bmatrix} 0 & -1 \\ \beta_{i1} & -\beta_{i2} \end{bmatrix}. \quad (7)$$

Now, for the case of a ring-road, we have $B \in \mathbb{R}^{n \times 1}$ and define:

$$J_2 = \begin{bmatrix} 0 & 1 \\ 0 & 0 \end{bmatrix}, \quad B_1 = \begin{bmatrix} 0 \\ 1 \end{bmatrix}, \quad B_2 = \begin{bmatrix} 0 \\ 0 \end{bmatrix}. \quad (8)$$

Moreover, for an open-road, we have $B \in \mathbb{R}^{n \times 2}$, and J_2 , B_1 , and B_2 are defined as:

$$J_2 = \begin{bmatrix} 0 & 0 \\ 0 & 0 \end{bmatrix}, \quad B_1 = \begin{bmatrix} 1 & 0 \\ 0 & 1 \end{bmatrix}, \quad B_2 = \begin{bmatrix} 0 & 0 \\ 0 & 0 \end{bmatrix}. \quad (9)$$

Finally, we note that the CAV can receive the state information associated with only a number of HDVs, due to its communications constraints. For example, in Fig. 1, the green links show HDVs whose information is available to the CAV. In this direction, an output vector $y(t) \in \mathbb{R}^{2m}$ is defined, that includes the states of the CAV together with the states of all HDVs whose information is accessible by the CAV. For $k = 1, \dots, m$, let j_k be the index of the vehicle whose state information, i.e. \bar{s}_{j_k} and \bar{v}_{j_k} , can be directly measured and observed. Consequently, we have:

$$y(t) = Cx(t), \quad (10)$$

where $C^T = [e_{(2*j_1-1)} \ e_{2*j_1} \ \dots \ e_{(2*j_m-1)} \ e_{2*j_m}]$. Note that we can have $j_1 = 1$, since the CAV has access to its own information.

In this paper, we design a dynamical output-feedback controller that has the following dynamics:

$$\begin{aligned} \dot{x}_k(t) &= A_k x_k(t) + B_k y(t) \\ u(t) &= C_k x_k(t) \end{aligned}, \quad (11)$$

where $A_k \in \mathbb{R}^{2n \times 2n}$, $B_k \in \mathbb{R}^{2n \times 2m}$ and $C_k \in \mathbb{R}^{1 \times 2m}$, and $x_k \in \mathbb{R}^{2n}$ is state of the controller.

Problem 1: In order to ensure the existence of an output-feedback controller, based on the separation principle [27], the first goal of this paper is to prove the stabilizability of pair (A, B) and detectability of pair (A, C) in (5) and (10).

Pair (A, B) is stabilizable if the uncontrollable modes are all stable. Similarly, pair (A, C) is detectable if the unobservable modes are all stable. We can use the Popov-Belevitch-Hautus

(PBH) test for checking the controllability and observability of a specific eigenvalue.

Property 1 ([44]): An eigenvalue λ of A for a pair (A, B) (resp., (A, C)) is controllable (resp., observable) if and only if for all nonzero ρ for which $\rho^T A = \lambda \rho^T$ (resp., $A \rho = \lambda \rho$), $\rho^T B \neq 0$ (resp., $C \rho \neq 0$).

Problem 2: The next problem of this work is dedicated to computing matrices A_k , B_k , C_k , and D_k in (11), for the mixed traffic system described in (5) and (10), such that the undesired perturbations in the traffic flow are dissipated. We first solve this problem without considering any uncertainty in the parameters of heterogeneous vehicles. Subsequently, we assume that there might be uncertainties in the dynamical model of HDVs, and we compute a robust output-feedback controller in the presence of disturbance and parametric uncertainty.

Accordingly, in the next section, we analyze the stabilizability and detectability of the mixed traffic system (5) and (10), and subsequently, we design a dynamic controller.

III. STABILIZABILITY AND DETECTABILITY

In this section, the stabilizability and detectability of dynamical system (5) and (10) are discussed.

A. Stabilizability Analysis

In order to prove the stabilizability of the mixed traffic system, we first consider a ring-road and prove that there is only one uncontrollable eigenvalue at the origin.

Property 2: In the case of a ring-road, the pair (A, B) in (5), where B is defined in (8), has only one uncontrollable eigenvalue at the origin.

Proof: Let $\rho = [\rho_1^T \ \dots \ \rho_n^T] \in \mathbb{R}^{2n}$, where $\rho_i^T = [\rho_{i1} \ \rho_{i2}]^T$. Considering the expression of A in (6), equation $\rho^T A = 0$ leads to

$$\begin{aligned} \rho_i^T A_{i2} + \rho_{i+1}^T A_{(i+1)1} &= 0, \quad i = 2, \dots, n-1 \\ \rho_1^T J_1 + \rho_2^T A_{21} &= 0 \\ \rho_1^T J_2 + \rho_n^T A_{n2} &= 0 \end{aligned}. \quad (12)$$

Now, from (12), one can derive

$$\begin{aligned} \rho_{i2} &= 0, \quad i = 2, \dots, n \\ \rho_{i1} &= \rho_{(i+1)1}, \quad i = 1, \dots, n-1. \end{aligned}$$

Thus, a left eigenvector ρ of A associated with $\lambda = 0$ can be written as $\rho = [\alpha, \beta, \alpha, 0, \dots, \alpha, 0]^T$. Now, assume that $\lambda = 0$ is an uncontrollable eigenvalue. Thus, from Proposition 1, one can see that $\rho^T B = 0$, which essentially means $\rho_{12} = 0$. Now, define $V_u = \{\rho \in \mathbb{R}^{2n} : \rho^T A = 0, \rho^T B = 0\}$. Then, one can see that $V_u = \{\rho \in \mathbb{R}^{2n} : \rho = [\alpha, 0, \alpha, 0, \dots, \alpha, 0]^T, \text{ for some } \alpha \neq 0\}$. Thus, $\dim(V_u) = 1$, which implies that there is only one uncontrollable eigenvalue of A at the origin. ■

Now, consider an open-road. Next, we show that in this case, there is no uncontrollable eigenvalue at the origin.

Property 3: In the case of an open-road, the pair (A, B) in (5), where B is defined in (9), has no uncontrollable eigenvalue at the origin.

Proof: In this case, from (12), we have:

$$\begin{aligned}\rho_{i2} &= 0, & i &= 2, \dots, n \\ \rho_{i1} &= \rho_{(i+1)1}, & i &= 1, \dots, n-1 \\ \rho_{n1} &= 0.\end{aligned}$$

Therefore, a nonzero left eigenvector ρ of A associated with $\lambda = 0$ has a form as $\rho = [0 \ \beta \ 0 \ \dots \ 0]^T$. Assume that we have an uncontrollable eigenvalue at the origin. Thus, from Proposition 1, $\rho^T B = 0$ leads to $\rho_{11} = \rho_{12} = 0$, implying that $\rho = 0$, that is a contradiction. ■

Next, it suffices to show that all unstable eigenvalues of A in (5), if any, are controllable.

Lemma 1: Let $\lambda \in \mathbb{C}$ with $\text{Re}(\lambda) > 0$, and for $i = 2, \dots, n$, let A_{i2} be defined as (7). Then, the matrix $(\lambda I - A_{i2})$ is nonsingular.

Proof: For $i = 2, \dots, n$, define $S_i(\lambda) = \det(\lambda I - A_{i2}) = \lambda^2 + \beta_{i2}\lambda + \beta_{i1}$. Based on this equation, the sum of eigenvalues of A_{i2} equals $-\beta_{i2}$, and their product is β_{i1} . If the roots of $S_i(\lambda)$ are real, then, since $\beta_{i1}, \beta_{i2} > 0$ from (2), both the roots are negative. Moreover, if the roots are complex and are written as $a + ib$ and $a - ib$, then since $2a = -\beta_{i2}$, we have $a < 0$. Therefore, because we have $\text{Re}(\lambda) > 0$, one can conclude that $S_i(\lambda) \neq 0$, implying that for $i = 2, \dots, n$, $(\lambda I - A_{i2})$ is nonsingular. ■

Theorem 1: For both cases of a ring-road and an open-road, the pair (A, B) associated with the mixed traffic system described in (5) is stabilizable.

Proof: Let λ be an eigenvalue of A with $\text{Re}(\lambda) > 0$, and let also $\rho = [\rho_1^T \ \dots \ \rho_n^T]^T \in \mathbb{R}^{2n}$ be its nonzero left eigenvector, where $\rho_i^T = [\rho_{i1} \ \rho_{i2}]$. Define $A_{11} = J_2$ and $A_{12} = J_1$. Then, for $i = 1, \dots, n$, equation $\rho^T A = \lambda \rho^T$ implies that

$$\rho_i^T (\lambda I - A_{i2}) = \rho_{i+1}^T A_{(i+1)1}. \quad (13)$$

Now, one can see that $\det(\lambda I - A_{12}) = \lambda^2$, which is nonzero, since $\lambda \neq 0$. Moreover, since $\text{Re}(\lambda) > 0$, Lemma 1 implies that $(\lambda I - A_{i2})$ is nonsingular. Accordingly, for $i = 1, \dots, n$, one can rewrite (13) as

$$\rho_i^T = \rho_{i+1}^T A_{(i+1)1} (\lambda I - A_{i2})^{-1}. \quad (14)$$

Let $L_i = (\lambda I - A_{i2})^{-1}$. Now, by recursively employing equation (14) for $i = 1, \dots, n$, we can derive

$$\begin{aligned}\rho_1^T &= \rho_2^T A_{21} L_1 \\ &= \rho_3^T A_{31} L_2 A_{21} L_1 \\ &= \dots \\ &= \rho_n^T A_{n1} L_{n-1} A_{(n-1)1} \dots L_2 A_{21} L_1 \\ &= \rho_1^T A_{11} (L_n A_{n1}) \dots (L_2 A_{21}) L_1.\end{aligned} \quad (15)$$

In the case an open-road, since $A_{11} = 0$, one can conclude from (15) that $\rho_1 = 0$. Now, we want to prove that $\rho = 0$ holds for a ring-road as well. Note that we have

$$L_i A_{i1} = \frac{1}{s_1^i} \begin{bmatrix} 0 & s_2^i \\ 0 & s_3^i \end{bmatrix}, \quad i = 2, \dots, n, \quad (16)$$

where $s_1^i = \lambda^2 + \beta_{i2}\lambda + \beta_{i1}$, $s_2^i = \lambda + \beta_{i2} - \beta_{i3}$, and $s_3^i = \beta_{i3}\lambda + \beta_{i1}$. As shown before, $s_1^i \neq 0$. Now, we substitute (16) into (15), and for the case of a ring-road, we obtain

$$[\rho_{11} \ \rho_{12}] = \frac{\prod_{i=2}^n s_3^i}{\lambda \prod_{i=2}^n s_1^i} [\rho_{11} \ \rho_{12}] \begin{bmatrix} 0 & 1 \\ 0 & 0 \end{bmatrix}. \quad (17)$$

Equation (17) leads to $\rho_{11} = 0$ and $\rho_{12} = \frac{\prod_{i=2}^n s_3^i}{\lambda \prod_{i=2}^n s_1^i} \rho_{11} = 0$. Thus, $\rho_1 = 0$. Now, for both cases of a ring-road and an open-road, by recursively applying (14) for $i = n, n-1, \dots, 2$, one can conclude that $\rho_i = 0$. Therefore, we have $\rho = 0$ that contradicts the assumption. Thus, A has no eigenvalue which lies on the right half-plane. In addition, from Proposition 2, for the case of a ring-road, there is only one uncontrollable eigenvalue at origin. Furthermore, Proposition 3 implies that in the case of an open-road, there is no uncontrollable eigenvalue at origin. Hence, in both cases, the system is stabilizable. ■

Remark 1: In [23], it has been stated that the mixed traffic system described in (5) is stabilizable if for all $i, k \in \{1, 2, \dots, n\}$, we have $\beta_{k1}^2 - \beta_{i2}\beta_{k1}\beta_{k3} + \beta_{i1}\beta_{k3}^2 \neq 0$. Moreover, through a different approach, it has been shown that there is only one uncontrollable eigenvalue at origin. However, in Theorem 1, without assuming any restrictive constraint, we have demonstrated the stabilizability of a mixed traffic system with heterogeneous HDVs for both cases of a ring-road and an open-road and proved that the system is stabilizable even if for some $i, k \in \{1, 2, \dots, n\}$, we have $\beta_{k1}^2 - \beta_{i2}\beta_{k1}\beta_{k3} + \beta_{i1}\beta_{k3}^2 = 0$.

B. Detectability Analysis

Here, the detectability of the mixed traffic system is studied, and we show that by observing only the states of the single CAV, the detectability of the whole system can be ensured.

Property 4: The zero eigenvalue of the mixed traffic system described in (5) and (10), in both cases of a ring-road and an open-road, is observable even if the CAV has access to only its own states.

Proof: Let $C = [e_1 \ e_2]$, and assume that $\lambda = 0$ is not observable. Then, from Proposition 1, A has a nonzero right eigenvector ρ , where we have both $A\rho = 0$ and $C\rho = 0$. Let $\rho = [\rho_1^T \ \dots \ \rho_n^T]^T \in \mathbb{R}^{2n}$, where $\rho_i^T = [\rho_{i1} \ \rho_{i2}]$. From equation $A\rho = 0$, one can write:

$$\begin{aligned}\rho_{i2} - \rho_{(i+1)2} &= 0, & i &= 2, \dots, n \\ \beta_{i3}\rho_{(i-1)2} + \beta_{i1}\rho_{i1} - \beta_{i2}\rho_{i2} &= 0, & i &= 2, \dots, n\end{aligned} \quad (18)$$

Moreover, from $C\rho = 0$, one can conclude that $\rho_{11} = \rho_{12} = 0$. Thus, (18) leads to $\rho = 0$ in both cases of a ring-road and an open-road, which is a contradiction. Therefore, the zero eigenvalue is observable. ■

Theorem 2: In the both cases of a ring-road and an open-road, the mixed traffic system described in (5) and (10) is detectable even if only the states of the single CAV are directly observed.

Proof: Let $C = [e_1 \ e_2]$. Assume that the system is not detectable. Then, A has an eigenvalue λ on the right half-plane with a nonzero right eigenvector ρ such that $C\rho = 0$. Denote $\rho = [\rho_1^T \ \dots \ \rho_n^T]^T \in \mathbb{R}^{2n}$, where $\rho_i^T = [\rho_{i1} \ \rho_{i2}]$. Then, we should have $\rho_{11} = \rho_{12} = 0$. Define $A_{11} = J_2$ and

$A_{12} = J_1$. Now, from equation $A\rho = \lambda\rho$, for $i = 1, \dots, n$, one can write:

$$(\lambda I - A_{i2})\rho_i = A_{i1}\rho_{i-1}.$$

Since $\text{Re}(\lambda) > 0$, from Lemma 1, one can see that, for $i = 2, \dots, n$, $(\lambda I - A_{i2})$ is invertible. Moreover, $\det(\lambda I - A_{12}) = \lambda^2 \neq 0$. Let $L_i = (\lambda I - A_{i2})^{-1}$. Then, for $i = 1, \dots, n$, we can write:

$$\rho_i = L_i A_{i1} \rho_{i-1}. \quad (19)$$

Now, since $\rho_1 = 0$, recursively using equation (19) for $i = 2, \dots, n$ leads to $\rho = 0$, which contradicts the assumption. In addition, based on Proposition 4, the zero eigenvalue is observable. Thus, in summary, one can conclude that the system is detectable. ■

IV. CONTROLLER SYNTHESIS: WITHOUT UNCERTAINTIES

In this section, we aim to design a dynamic output-feedback controller for the mixed traffic system (5) to dissipate undesired perturbations. In the first step, we assume there is no uncertainty in the model of the traffic system and design an output-feedback controller.

A. Disturbances and Performance Outputs

In fact, the perturbations may appear due to lane changes or merges or the stochastic behavior of HDVs in ring-roads with no bottlenecks [8], [23].

Perturbations are modeled as disturbance signals added to the acceleration of each vehicle. Thus, by defining $d = [d_1(t) \dots d_n(t)]^T \in \mathbb{R}^n$ as the disturbance vector and the matrix

$$B_d = \begin{bmatrix} b_d & 0 & \dots & 0 \\ 0 & b_d & \dots & \vdots \\ \vdots & \ddots & \ddots & 0 \\ 0 & \dots & 0 & b_d \end{bmatrix} \in \mathbb{R}^{2n \times n},$$

with $b_d = [0, 1]^T$, the dynamics of the mixed traffic system in the presence of disturbances can be written as

$$\begin{aligned} \dot{x}(t) &= Ax(t) + Bu(t) + B_d d(t) \\ z(t) &= C_z x(t) + D_z u(t), \\ y(t) &= Cx(t) \end{aligned} \quad (20)$$

where for the case of a ring-road, one can define the controlled output (performance output) $z(t) \in \mathbb{R}^{2n+1}$ as

$$z(t) = [\gamma_s \bar{s}_1(t) \quad \gamma_v \bar{v}_1 \quad \dots \quad \gamma_s \bar{s}_n(t) \quad \gamma_v \bar{v}_n \quad \gamma_u u]^T. \quad (21)$$

The parameters $\gamma_s, \gamma_v, \gamma_u > 0$ denote the penalties associated with the spacing error, the velocity deviation, and the control energy, respectively. Thus, $C_z = [\mathcal{T}^{\frac{1}{2}} \quad 0_{2n \times 1}]^T$ includes the weights of the states, with $\mathcal{T}^{\frac{1}{2}} = \text{diag}(\gamma_s, \gamma_v, \dots, \gamma_s, \gamma_v)$, and $D_z = [0_{1 \times 2n} \quad \mathcal{Q}^{\frac{1}{2}}]^T$ is the weight of the control input, with $\mathcal{Q}^{\frac{1}{2}} = \gamma_u$. In the case of an open-road, we define $z(t) = [\gamma_s \bar{s}_1(t) \quad \gamma_v \bar{v}_1 \quad \dots \quad \gamma_s \bar{s}_n(t) \quad \gamma_v \bar{v}_n \quad \gamma_{u_1} u_1 \quad \gamma_{u_2} u_2]^T \in \mathbb{R}^{2n+2}$. In this case, one has $C_z = [\mathcal{T}^{\frac{1}{2}} \quad 0_{2n \times 2}]^T$ and $D_z = [0_{2 \times 2n} \quad \mathcal{Q}^{\frac{1}{2}}]^T$, with $\mathcal{Q}^{\frac{1}{2}} = \text{diag}(\gamma_{u_1}, \gamma_{u_2})$.

B. Output-feedback controller

Consider an output-feedback controller with the dynamics described in (11). We aim to design a dynamic controller that stabilizes the system (20) and minimizes the influence of the disturbance d on the performance output z .

By applying the controller (11) to (20), the closed-loop system is expressed as

$$\begin{aligned} \dot{\bar{x}}(t) &= \bar{A}\bar{x}(t) + \bar{B}d(t) \\ z(t) &= \bar{C}\bar{x}(t) \end{aligned}, \quad (22)$$

where $\bar{x} = \begin{bmatrix} x(t) \\ x_k(t) \end{bmatrix}$, $\bar{A} = \begin{bmatrix} A & BC_k \\ B_k C & A_k \end{bmatrix}$, $\bar{B} = \begin{bmatrix} B_d \\ 0 \end{bmatrix}$ and $\bar{C} = [C_z \quad D_z C_k]$.

C. H_∞ Control Problem

Let T_{zd} be the closed-loop transfer function from the disturbance d to the performance output z .

Problem: Find the matrices A_k , B_k , and C_k for the controller (11) such that the closed-loop system (22) satisfies the inequality

$$\|T_{zd}\|_\infty = \max_{d(t) \neq 0} \frac{\|z(t)\|_2}{\|d(t)\|_2} < \gamma, \quad (23)$$

and $\gamma > 0$ is minimized.

Note that $\|T_{zd}\|_\infty$ denotes the H_∞ norm of T_{zd} , which measures the largest input-output gain for energy or power input signals [45].

Problem solution: Based on the bounded real lemma (BRL) [46], $\|T_{zd}\|_\infty$ is smaller than γ if and only if there exists a positive definite matrix $P \succ 0$, and matrices A_k , B_k , and C_k satisfying

$$\begin{bmatrix} \bar{A}^T P + P \bar{A} & P \bar{B} & \bar{C}^T \\ \bar{B}^T P & -\gamma^2 I & 0 \\ \bar{C} & 0 & -I \end{bmatrix} \prec 0. \quad (24)$$

Now, note that the inequality (24) is not a linear matrix inequality (LMI) with respect to the variables P , A_k , B_k , and C_k , because it is not linear with respect to these variables. In order to extract an LMI for computing the controller parameters A_k , B_k , and C_k , we apply a method that has been presented in [45] in details, and we provide a summarized description of this method in the following.

Let us partition the matrices P and P^{-1} as the following form:

$$P = \begin{bmatrix} Y & N \\ N^T & * \end{bmatrix}, \quad P^{-1} = \begin{bmatrix} X & M \\ M^T & * \end{bmatrix},$$

where $X, Y \in \mathbb{R}^{2n \times 2n}$. Note that since $P \succ 0$, we have $X, Y \succ 0$. From the equation $PP^{-1} = I$, one can deduce that $NM^T + YX = I$. Further, one can find that $P = \Lambda_2 \Lambda_1^{-1}$, where

$$\Lambda_1 = \begin{bmatrix} X & I \\ M^T & 0 \end{bmatrix}, \quad \Lambda_2 = \begin{bmatrix} I & Y \\ 0 & N^T \end{bmatrix}.$$

Therefore, we have

$$\Lambda_1^T P \Lambda_1 = \Lambda_1^T \Lambda_2 = \begin{bmatrix} X & I \\ I & Y \end{bmatrix} \succ 0.$$

Substituting $P = \Lambda_2 \Lambda_1^{-1}$ in (24), we obtain

$$\Omega_1 = \begin{bmatrix} \bar{A}^T \Lambda_2 \Lambda_1^{-1} + \Lambda_1^{-T} \Lambda_2^T \bar{A} & \Lambda_1^{-T} \Lambda_2^T \bar{B} & \bar{C}^T \\ \bar{B}^T \Lambda_2 \Lambda_1^{-1} & -\gamma^2 I & 0 \\ \bar{C} & 0 & -I \end{bmatrix} \prec 0. \quad (25)$$

Now, let us define a matrix Ω_2 by the following congruent transformation of Ω_1

$$\begin{aligned} \Omega_2 &= \begin{bmatrix} \Lambda_1^T & 0 & 0 \\ 0 & I & 0 \\ 0 & 0 & I \end{bmatrix} \Omega_1 \begin{bmatrix} \Lambda_1 & 0 & 0 \\ 0 & I & 0 \\ 0 & 0 & I \end{bmatrix} \\ &= \begin{bmatrix} \Lambda_1^T \bar{A}^T \Lambda_2 + \Lambda_2^T \bar{A} \Lambda_1 & \Lambda_2^T \bar{B} & \Lambda_1^T \bar{C}^T \\ \bar{B}^T \Lambda_2 & -\gamma^2 I & 0 \\ \bar{C} \Lambda_1 & 0 & -I \end{bmatrix} \prec 0. \end{aligned} \quad (26)$$

Now, substituting the values of Λ_1 , Λ_2 , \bar{A} , \bar{B} and \bar{C} , we obtain the following matrix inequality:

$$\Omega_2 = \begin{bmatrix} \Omega_{11} & \Omega_{12} & \Omega_{13} & \Omega_{14} \\ \Omega_{21} & \Omega_{22} & \Omega_{23} & \Omega_{24} \\ \Omega_{31} & \Omega_{32} & \Omega_{33} & \Omega_{34} \\ \Omega_{41} & \Omega_{42} & \Omega_{43} & \Omega_{44} \end{bmatrix} \prec 0, \quad (27)$$

where

$$\begin{aligned} \Omega_{11} &= AX + XA^T + BC_k M^T + MC_k^T B^T \\ \Omega_{12} &= \Omega_{21}^T = MA_k^T N^T + XC^T B_k^T N^T + MC_k^T B^T Y \\ &\quad + XA^T Y + A \\ \Omega_{22} &= A^T Y + Y A + NB_k C + C^T B_k^T N^T \\ \Omega_{13} &= \Omega_{31}^T = B_d, \quad \Omega_{14} = \Omega_{41}^T = XC_z^T + MC_k^T D_z^T, \\ \Omega_{23} &= \Omega_{32}^T = Y B_d, \quad \Omega_{24} = \Omega_{42}^T = C_z^T, \quad \Omega_{33} = -\gamma^2 I, \\ \Omega_{34} &= \Omega_{43} = 0, \quad \Omega_{44} = -I. \end{aligned}$$

Finally, by defining a new set of variables as

$$\begin{aligned} \hat{A} &= NA_k M^T + NB_k CX + YBC_k M^T + YAX \\ \hat{B} &= NB_k \\ \hat{C} &= C_k M^T \\ \eta &= \gamma^2 \end{aligned}, \quad (28)$$

we obtain the LMIs described in (29) with respect to variables η , X , Y , \hat{A} , \hat{B} , \hat{C} . Therefore, if the optimization problem (29) is feasible, then we can find η , X , Y , \hat{A} , \hat{B} , and \hat{C} and solve the matrix equation $NM^T = I - YX$ for the non-singular matrices M and N . Moreover, matrices A_k , B_k , and C_k in the state-space realization of the output-feedback controller can be derived based on (28) as follows:

$$\begin{aligned} A_k &= N^{-1}(\hat{A} - NB_k CX - YBC_k M^T - YAX)M^{-T}, \\ B_k &= N^{-1}\hat{B}, \\ C_k &= \hat{C}M^{-T}. \end{aligned} \quad (30)$$

V. CONTROLLER SYNTHESIS: WITH UNCERTAINTIES

In this section, we consider parametric uncertainties in the dynamic model of the HDVs. In fact, we assume that β_{i1} , β_{i2} , and β_{i3} , appearing in (7), are unknown parameters for the mixed traffic system. Then, we synthesize an output-feedback

controller with dynamics (11) that stabilizes the entire closed-loop system in the presences of disturbances and parametric uncertainties.

After the linearization of the overall dynamics of the system, the uncertainty is assumed to appear in the system matrix A in (6) as

$$A = A_{\mathcal{N}} + \Delta A. \quad (31)$$

The matrix $A_{\mathcal{N}}$ is the mean-valued matrix that is constant and known. One can calculate $A_{\mathcal{N}}$ as $A_{\mathcal{N}} = \left[\frac{a_{ij,\min} + a_{ij,\max}}{2} \right]$, where $a_{ij,\min}$ (resp., $a_{ij,\max}$) is the minimum (resp., maximum) value that an entry of A in its i th row and j th column can have. On the other hand, ΔA represents parametric uncertainties, that is assumed to be structurally bounded. One can write ΔA as

$$\Delta A = LFR,$$

where the matrices $L \in \mathbb{R}^{2n \times 2n}$ and $R \in \mathbb{R}^{2n \times 2n}$ are known constant matrices. Moreover, $F \in \mathbb{R}^{2n \times 2n}$ is an unknown matrix, which satisfies the following condition:

$$F^T F \preceq I. \quad (32)$$

Remark 2: (Computing L and R) We can choose L and R as $L = \rho I$ and $R = \rho I$. Therefore, $\Delta A = LFR = \rho \rho F$, and based on Fact 1, we get $\|F\| = (\rho \rho)^{-1} \|\Delta A\| \leq (\rho \rho)^{-1} \|\Delta A\|_{\mathcal{F}}$. On the other hand, $\Delta A = A - A_{\mathcal{N}} = [\tilde{a}_{ij}]$, where $|\tilde{a}_{ij}| \leq \frac{1}{2}(a_{ij,\max} - a_{ij,\min})$. Therefore, $\|F\| \leq (2\rho \rho)^{-1} (\sum_{i=1}^{2n} \sum_{j=1}^{2n} (a_{ij,\max} - a_{ij,\min})^2)^{\frac{1}{2}}$. Now, if one sets $\rho \rho = \frac{1}{2} (\sum_{i=1}^{2n} \sum_{j=1}^{2n} (a_{ij,\max} - a_{ij,\min})^2)^{\frac{1}{2}}$, then $\|F\| \leq 1$, and the condition (32) is satisfied.

In the following, we show how we can ensure the existence of an output-feedback controller that attenuates the effect of the disturbance on the performance output, while stabilizing the closed-loop system.

Theorem 3: Consider a system with dynamics (20), which has uncertainties that are modelled as (31). Then, there exists an output-feedback controller that stabilizes the closed-loop system (22) and minimizes γ in the inequality (23) if the optimization problem (33) feasible.

Proof of Theorem 3: See Appendix.

Remark 3: By solving the optimization problem (33), η , ϵ_1 , ϵ_2 , ϵ_3 , \hat{A} , \hat{B} , \hat{C} , X , and Y can be computed. We note that $\eta = \gamma^2$, where γ is an upper bound of the $\|T_{zd}\|_{\infty}$. In addition, we can solve the matrix equation $NM^T = I - YX$ for the non-singular matrices M and N . Then, the matrices A_k , B_k , and C_k in the state-space realization of the output-feedback controller can be obtained as

$$\begin{aligned} A_k &= N^{-1}(\hat{A} - NB_k CX - YBC_k M^T - Y A_{\mathcal{N}} X)M^{-T} \\ B_k &= N^{-1}\hat{B} \\ C_k &= \hat{C}M^{-T}. \end{aligned}$$

VI. SIMULATION RESULTS

In this section, the efficiency of the proposed control strategies are validated through numerical simulations. The minimization problems (29) and (33) are solved in YALMIP interface for MATLAB with Sedumi solver. For a better comparison of the results, we simulate an experimental setup

$$\begin{aligned}
& \min_{\eta, X, Y, \hat{A}, \hat{B}, \hat{C}} \eta \\
& \text{subject to:} \\
& \begin{bmatrix} X & I \\ I & Y \end{bmatrix} \succ 0 \\
& \begin{bmatrix} AX + XA^T + B\hat{C} + \hat{C}^T B^T & \hat{A}^T + A & B_d & XC_z^T + \hat{C}^T D_z^T \\ * & A^T Y + YA + \hat{B}C + C^T \hat{B}^T & YB_d & C_z^T \\ * & * & -\eta I & 0 \\ * & * & * & -I \end{bmatrix} \prec 0
\end{aligned} \tag{29}$$

$$\begin{aligned}
& \min_{\eta, \epsilon_1, \epsilon_2, \epsilon_3, X, Y, \hat{A}, \hat{B}, \hat{C}} \eta \\
& \text{subject to:} \\
& \begin{bmatrix} X & I \\ I & Y \end{bmatrix} \succ 0 \\
& \begin{bmatrix} \Gamma_{11} & \Gamma_{12} \\ * & \Gamma_{22} \end{bmatrix} \prec 0 \\
& \Gamma_{11} = \begin{bmatrix} A_N X + XA_N^T + B\hat{C} + \hat{C}^T B^T + L(\epsilon_1 + \epsilon_2)L^T & \hat{A}^T + A_N & B_d & XC_z^T + \hat{C}^T D_z^T \\ * & A_N^T Y + YA_N + \hat{B}C + C^T \hat{B}^T + \epsilon_3 R^T R & YB_d & C_z^T \\ * & * & -\eta I & 0 \\ * & * & * & -I \end{bmatrix} \\
& \Gamma_{12} = \begin{bmatrix} XR^T & 0 & 0 & YL & 0 \\ 0 & R^T & YL & 0 & XR^T \\ 0 & 0 & 0 & 0 & 0 \\ 0 & 0 & 0 & 0 & 0 \end{bmatrix} \\
& \Gamma_{22} = -\text{diag}(\epsilon_1 I, \epsilon_2 I, \epsilon_3 I, I, I)
\end{aligned} \tag{33}$$

that is similar to the ones considered in [28], [23], where a ring-road with a circumference $D = 400$ m and 20 vehicles has been studied (since the results for the case of an open-road is analogous to the case of a ring-road, we illustrate here the simulation results only for a ring-road). We assume that the 1st vehicle can be a CAV that has access to the state information of the five HDVs ahead and the five HDVs behind.

A. Simulation setup

Through using an optimal velocity model (OVM), any nonlinear function $H_i(\cdot)$ in (1), $i = 2, \dots, 20$, that describes the acceleration function of the i th HDV is written as $H_i(\cdot) = \alpha_i(\mathcal{V}_i(s_i(t)) - v_i(t)) + \theta_i \dot{s}_i(t)$, where α_i and θ_i are sensitivity coefficient in an OVM. Moreover, $\mathcal{V}_i(s_i)$ is the desired speed of HDV i that is a function of spacing s_i . Due to heterogeneity of HDVs, we set $\alpha_i = 0.6 + U[-0.1, 0.1]$ and $\theta_i = 0.9 + U[-0.1, 0.1]$, where $U[a, b]$ represents a uniform distribution function that take values from the interval $[a, b]$. Moreover, we define $\mathcal{V}_i(s_i)$ as a piecewise function

$$\mathcal{V}_i(s_i) = \begin{cases} 0, & s_i \leq s_{i,st}, \\ h_{i,v}(s_i), & s_{i,st} < s_i < s_{i,go}, \\ v_{i,max}, & s_i \geq s_{i,go}, \end{cases}$$

where we set $s_{i,st} = 5$, $s_{i,go} = 35 + U[-5, 5]$, $v_{i,max} = 30$, and $h_{i,v}(s_i)$ is a nonlinear function chosen as [31]

$$h_{i,v}(s_i) = \frac{v_{i,max}}{2} (1 - \cos(\pi \frac{s_i - s_{i,st}}{s_{i,go} - s_{i,st}})).$$

In order to ensure the safety and prevent collisions, every vehicle is also assumed to be equipped with an automatic braking system, described as

$$\dot{v}(t) = a_{\min} \quad \text{if} \quad \frac{v_i^2(t) - v_{i-1}^2(t)}{2s_i(t)} \geq |a_{\min}|,$$

where $a_{\min} = -5$ m/s². Moreover, we set the maximum acceleration of any vehicle as $a_{\max} = 2$ m/s².

B. Stabilizability Verification

As the first scenario, assume that all vehicles are randomly distributed along the ring-road and start their movement with initial velocity $v_i(0)$ from the distribution $15 + U[-4, 4]$ m/s. Notice that we consider no uncertainties in the dynamic model of the system in this case. First, assume that all vehicles of the mixed traffic system are HDVs. In Fig. 2(a), it can be seen that multiple perturbations occur in this system, which are amplified over time and generate an unstable nonlinear wave moving upstream the traffic flow.

Next, assume that the 1st vehicle is a CAV that is controlled by an output-feedback controller described in Section IV-C.

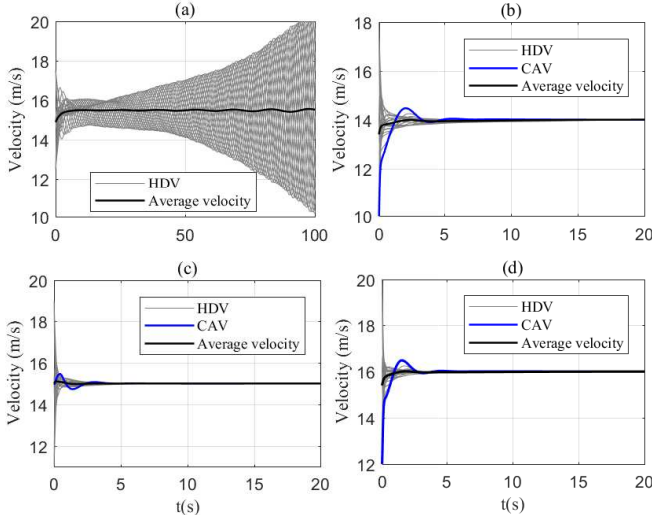


Fig. 2. (a) Velocity profile of vehicles when they are all HDVs; (b)–(d) Velocity profile of vehicles when the 1st vehicle is a CAV under the proposed control in Section IV-C, and v^* is 15, 16, and 14 for (b), (c), and (d), respectively.

First, we set the equilibrium velocity as $v^* = 15$ m/s. Then, the equilibrium spacing of vehicle i is obtained by solving the equation $0 = H_i(15, s_i^*, 0)$. Note that in a circular path, the sum of spacing of all vehicles should equal to the circumference D . In other words, we should have $\sum_{i=1}^2 s_i(t) = \sum s_i^* = 400$. Now, one can see in Fig. 2(b) that the perturbations can be attenuated within a short time. As the next experiments, we change the equilibrium velocity to 16 m/s and 14 m/s, respectively. Notice that in this case, the parameters of the linearized system (5) that are computed around the equilibrium point will be changed. In these two cases, one can observe in Figs. 2(c,d) that the single CAV is still capable of stabilizing traffic flow and steering it towards the new equilibrium points, which verifies the stabilizability of the mixed traffic system with a single CAV.

C. Robustness Against Disturbances

In this part, we aim to illustrate the performance of the output-feedback controller, proposed in Section IV-C, to dampen the undesired disturbances.

We note that the parameters γ_s , γ_v , and γ_u in the performance output $z(t)$ in (21), should be selected such that the optimization problem (29) is feasible. Moreover, we should prevent rapid oscillations in the output of the system. If we choose smaller values for the parameters γ_s and γ_v , the system oscillations increase, while the system response converges more slowly that is not desirable. As a result, there is a trade-off between the convergence rate of the system response and its quality in terms of the amplitude of the oscillations. Accordingly, adjusting the values of the parameters γ_s and γ_v is an important part of the controller design. In order to have an appropriate output behaviour of the traffic flow system, we choose $\gamma_s = 0.03$, $\gamma_v = 0.15$, and $\gamma_u = 1$.

As the next experiment, we assume that, at $t = 20$ s, the 7th vehicle is decelerated at -3 m/s² for 3 s (this perturbation can

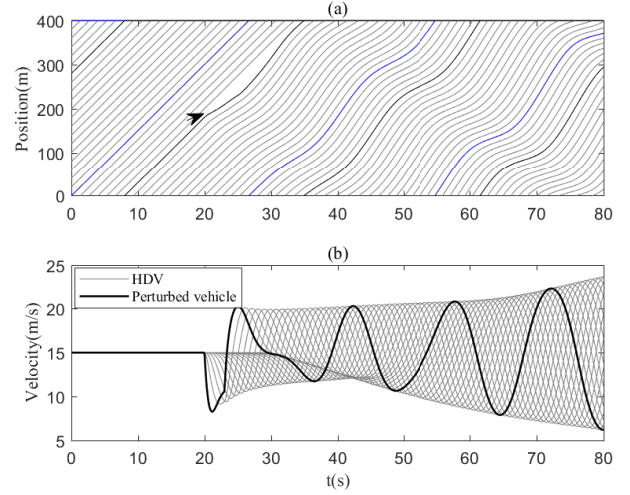


Fig. 3. (a) Trajectory of all vehicles (the trajectory of the perturbed vehicle and vehicle no. 20 are, respectively, shown by black and blue lines) when there is no CAV in the platoon (a disturbance is added to the acceleration of vehicle 7 at $t = 20$ s); (b) Velocity profile of vehicles.

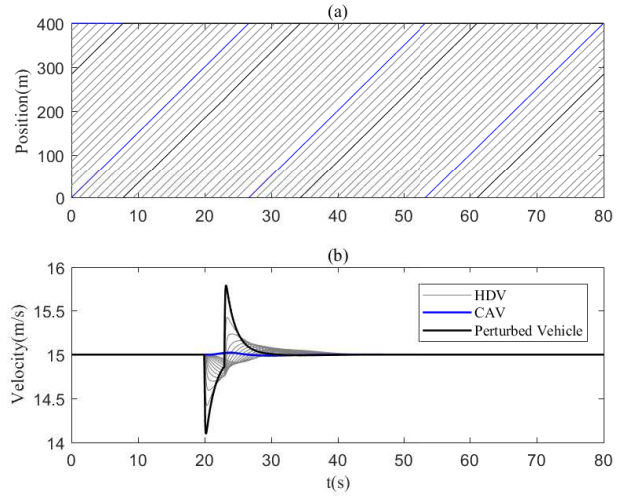


Fig. 4. (a) Trajectory of all vehicles (the trajectory of the perturbed vehicle and vehicle no. 20 are, respectively, shown by black and blue lines) when there is one CAV under the proposed control in Section IV-C (a disturbance is added to the acceleration of vehicle 7 at $t = 20$ s); (b) Velocity profile of vehicles.

be due to road bottlenecks). In Figs. 3 (a,b), the trajectory and the velocity profile of all vehicles when there is no CAV in the system are illustrated. One can see in these figures that the perturbation does not vanish, and a nonlinear wave appears that propagates against the traffic flow. On the other hand, when one CAV is added to the traffic system and is controlled by the proposed strategy in Section IV-C, one can see in Figs. 4 (a,b) that the stop-and-go-wave can be quickly dissipated, and the traffic flow is stabilized to the equilibrium point.

D. Comparison with Existing Results

In this part, we compare the efficiency of the output-feedback controller proposed in Section IV-C with some of the existing control strategies in the literature. In particular, we

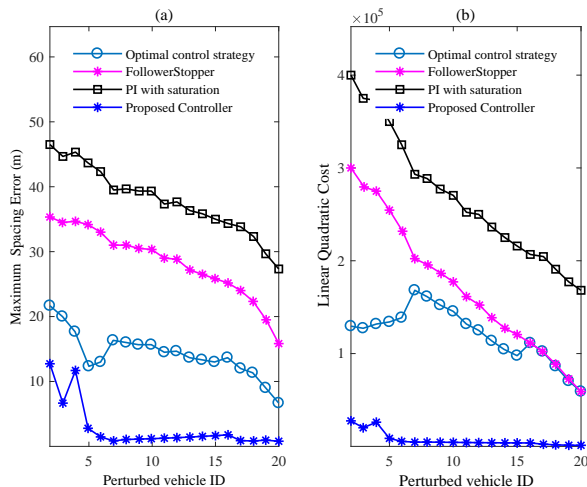


Fig. 5. Comparison of the results for four different control strategies; (a) $\max_t |s_1(t) - s_1^*|$ w.r.t. the index of the perturbed HDV; (b) Energy of the performance output, i.e., $\|z(t)\|_2 = \int_{t=0}^{\infty} x^T(t)\mathcal{T}x(t) + u^T(t)\mathcal{Q}u(t)$, w.r.t. the index of the perturbed HDV.

compare our result with an optimal control strategy proposed in [23] and the two heuristic control methods presented in [12], that is, Follower-Stopper and PI with Saturation.

At any stage of the new experiment, we assume that one of the HDVs is decelerated at -3 m/s^2 for 3 s. Thus, the disturbance signal is a pulse with a time duration of 3 s and an amplitude of -3 m/s^2 . The initial velocity of all vehicles is also 15 m/s.

In Fig. 5 (a), after applying different control strategies, we illustrate the maximum absolute value of the spacing error during the overall process with respect to the index of a single perturbed HDV. Then, one can observe that with our proposed controller, the absolute value of the spacing error is much less than the two heuristic methods [12] and the optimal control strategy in [23]. In fact, with our controller, the spacing remains close to the equilibrium spacing over the whole process, and its fluctuations around the desired spacing are considerably smaller compared to the other strategies.

Another performance measure, in Fig. 5 (b), associated with any control strategy, a linear quadratic cost that is defined as the energy of the performance output $z(t)$ in (21) with respect to the different position of the perturbation is illustrated. As is evident in this figure, thanks to considering a system-level performance, our control methodology not only leads to a much better efficiency compared to the heuristic strategies in [12], but it has also a substantially smaller cost than the optimal controller proposed in [23]. In fact, in [23], a sub-optimal solution for synthesizing a static controller has been developed, while in this work, a global optimal dynamic controller with more degrees of freedom is designed.

E. Robustness against Disturbances and Uncertainties

As the last experiment, we assume that some parameters appearing in the dynamic model of HDVs are uncertain. However, in our case study, the nominal values of the parameters

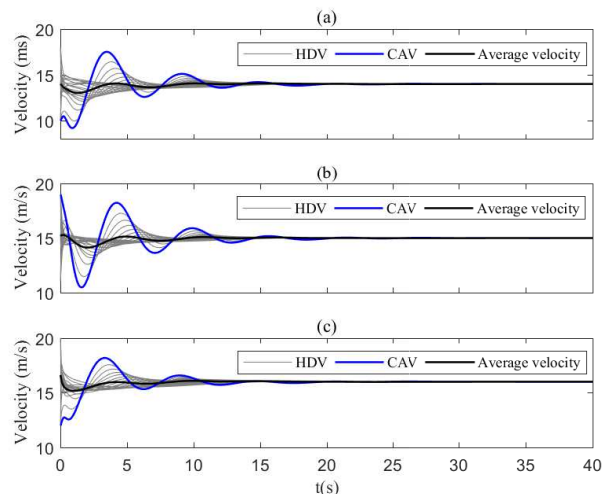


Fig. 6. (a)–(c) Velocity profile of vehicles when there is one CAV under the proposed control in Section V in the presence of disturbances and the parametric uncertainties, and v^* is 14, 15, and 16 m/s for (a), (b), and (c), respectively.

are the same for all HDVs. In fact, instead of considering heterogeneous HDVs, we assume that there are a number of vehicles with homogeneous nominal dynamic models that may also include uncertainties. In order to dampen the perturbations of the mixed traffic system in the presence of parametric uncertainties, we design an output-feedback controller, using the procedure proposed in Section V.

In this experiment, we assume that the parameters α_i , θ_i , and $s_{i,go}$ (see Section VI-A) are unknown. The uncertain parameters are distributed around the nominal values $\alpha_N = 0.6$, $\theta_N = 0.9$, and $s_{N,go} = 35$. Then, one can define $\alpha_i = \alpha_N + \Delta\alpha$, $\theta_i = \theta_N + \Delta\theta$, $s_{i,go} = s_{N,go} + \Delta s_{go}$, where $-0.1 \leq \Delta\alpha \leq 0.1$, $-0.1 \leq \Delta\theta \leq 0.1$, and $-5 \leq \Delta s_{go} \leq 5$.

We first assume in this experiment that the initial velocity of the vehicles is randomly chosen from the distribution $15 + U[-4, 4] \text{ m/s}$. We compute the controller parameters associated with three different equilibrium velocities, that is, 14, 15, and 16 m/s. As observed in Figs. 6 (a–c), in these three cases, by using the control strategy proposed in Section V, the perturbations occurring in the traffic flow system are dampened, and the velocities of all vehicles converge to the equilibrium points within a short time.

Next, we assume that, at $t = 20 \text{ s}$, the vehicle no. 7 brakes at -3 m/s^2 for 3 s, and the single CAV is under the proposed control in Section V. In Fig. 7 (a,b), the velocity profile of all vehicles from a 3-dimensional (3D) and 2-dimensional (2D) perspective are illustrated. One can see that with the proposed output-feedback controller, the perturbation is attenuated very quickly in this traffic system. Moreover, as observed in Fig. 8, the spacing of HDVs and the CAV from the preceding vehicles converges to the equilibrium value in a few seconds.

VII. CONCLUSION

In this work, the stabilizability and detectability of a mixed traffic system along a ring-road and an open-road has been studied and analyzed. It has been shown that in both cases,

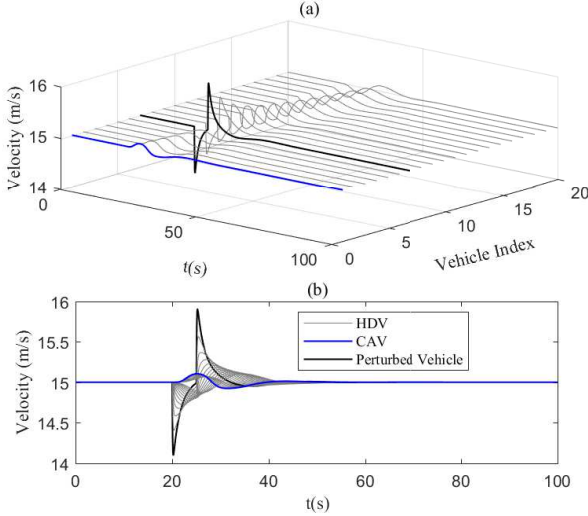


Fig. 7. (a)–(b) Velocity profile of all vehicles over time from 3D and 2D perspectives in the presence of disturbances and parametric uncertainties when the single CAV is under the proposed control in Section V (the blue (resp., black) line represents the spacing of the CAV (resp., the perturbed vehicle), i.e. $s_1(t)$ (resp., $s_7(t)$), and the grey lines denote the spacing of other HDVs).

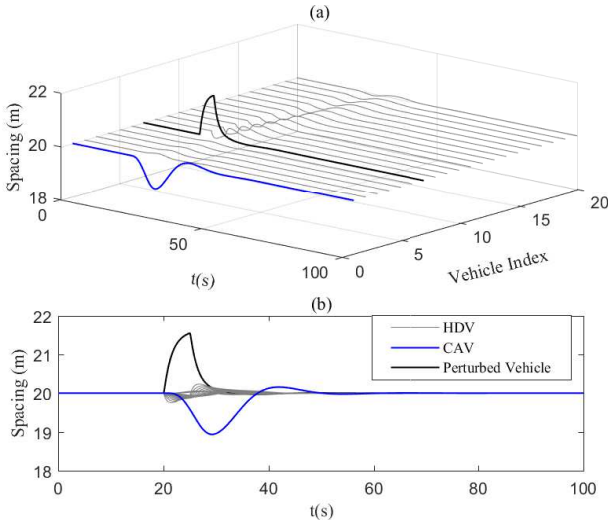


Fig. 8. (a)–(b) Spacing profile of all vehicles over time from 3D and 2D perspective in the presence of disturbances and parametric uncertainties when the single CAV is under the proposed control in Section V (the blue (resp., black) line represents the spacing of the CAV (resp., the perturbed vehicle), i.e. $s_1(t)$ (resp., $s_7(t)$), and the grey lines denote the spacing of other HDVs).

the system under investigation is stabilizable when there is one single CAV in the platoon. Moreover, we have demonstrated that the system is detectable even if the state information of only one vehicle is directly measured. Furthermore, by considering limited communication ability of the CAV to receive state information from its neighboring vehicles, an H_∞ dynamic output-feedback controller has been designed, that can provably smoothen the traffic flow even in the presences of abrupt and large disturbances (e.g. sharp deceleration downstream). We have also presented an H_∞ control method in the presence of parametric uncertainties in the dynamics of HDVs. The effectiveness of the proposed methods to achieve traffic flow stability has been verified and demonstrated through nu-

merical simulation experiments. Finally, the numerical results are compared to another approach from the literature. Future work is going to deal with the generalization of these results to more complex traffic patterns.

APPENDIX

We first present two results that will be used in the proof of Theorem 3 and then discuss the proof.

Lemma 2: [47] (Young inequality) Given matrices D, F , and S of appropriate dimensions, the inequality $DFS + (DFS)^T \preceq \epsilon^{-1}DD^T + \epsilon S^T S$ holds for some scalar $\epsilon > 0$ if we have $F^T F \preceq I$.

Lemma 3: [48] (Schur complement) Consider the matrices W_1, W_2 , and W_3 with the appropriate dimensions, where $W_1 = W_1^T \succ 0$. Then, the matrix inequality $W_1 + W_3^T W_2^{-1} W_3 \prec 0$ is equivalent to

$$\begin{bmatrix} W_1 & W_3^T \\ W_3 & -W_2 \end{bmatrix} \prec 0.$$

Proof of Theorem 3: As shown in section (IV-C), based on the bounded real lemma (BRL), if the matrix inequality (27) is satisfied, then $\|T_{zd}\|_\infty < \gamma$. Incorporating A from (31) to (27), we get

$$\Omega_4 = \Omega_3 + \Delta\Omega \prec 0,$$

where

$$\Omega_3 = \begin{bmatrix} \Omega_{11} & \Omega_{12} & \Omega_{13} & \Omega_{14} \\ \Omega_{21} & \Omega_{22} & \Omega_{23} & \Omega_{24} \\ \Omega_{31} & \Omega_{32} & \Omega_{33} & \Omega_{34} \\ \Omega_{41} & \Omega_{42} & \Omega_{43} & \Omega_{44} \end{bmatrix},$$

with

$$\begin{aligned} \Omega_{11} &= A_N X + X A_N^T + B C_k M^T + M C_k^T B^T, \\ \Omega_{12} &= \Omega_{21}^T = M A_k^T N^T + X C^T B_k^T N^T + M C_k^T B^T Y, \\ &\quad + X A_N^T Y + A_N \\ \Omega_{22} &= A_N^T Y + Y A_N + N B_k C + C^T B_k^T N^T, \\ \Omega_{13} &= \Omega_{31}^T = B_d, \quad \Omega_{14} = \Omega_{41}^T = X C_z^T + M C_k^T D_z^T, \\ \Omega_{23} &= \Omega_{32}^T = Y B_d, \quad \Omega_{24} = \Omega_{42}^T = C_z^T, \quad \Omega_{33} = -\gamma^2 I, \\ \Omega_{34} &= \Omega_{43} = 0, \quad \Omega_{44} = -I, \end{aligned}$$

and

$$\Delta\Omega = \begin{bmatrix} \Delta A X + X \Delta A^T & \Delta A + X \Delta A^T Y & 0 & 0 \\ \Delta A^T + Y \Delta A X & \Delta A^T Y + Y \Delta A & 0 & 0 \\ 0 & 0 & 0 & 0 \\ 0 & 0 & 0 & 0 \end{bmatrix}.$$

By substituting $\Delta A = LFR$, and applying condition (32) and Lemma 2, Ω_4 can be bounded as

$$\Omega_4 \preceq \Omega_3 + \sum_{i=1}^4 \Upsilon_i \prec 0,$$

where

$$\begin{aligned}\Upsilon_1 &= \begin{bmatrix} L \\ 0 \\ 0 \\ 0 \end{bmatrix} \epsilon_1 [L^T \ 0 \ 0 \ 0] + \begin{bmatrix} XR^T \\ 0 \\ 0 \\ 0 \end{bmatrix} \epsilon_1^{-1} [RX \ 0 \ 0 \ 0], \\ \Upsilon_2 &= \begin{bmatrix} L \\ 0 \\ 0 \\ 0 \end{bmatrix} \epsilon_2 [L^T \ 0 \ 0 \ 0] + \begin{bmatrix} 0 \\ R^T \\ 0 \\ 0 \end{bmatrix} \epsilon_2^{-1} [0 \ R \ 0 \ 0], \\ \Upsilon_3 &= \begin{bmatrix} XR^T \\ 0 \\ 0 \\ 0 \end{bmatrix} \delta [RX \ 0 \ 0 \ 0] + \begin{bmatrix} 0 \\ YL \\ 0 \\ 0 \end{bmatrix} \delta^{-1} [0 \ L^T Y \ 0 \ 0], \\ \Upsilon_4 &= \begin{bmatrix} 0 \\ R^T \\ 0 \\ 0 \end{bmatrix} \epsilon_3 [0 \ R \ 0 \ 0] + \begin{bmatrix} 0 \\ YL \\ 0 \\ 0 \end{bmatrix} \epsilon_3^{-1} [0 \ L^T Y \ 0 \ 0].\end{aligned}$$

Now, by defining $\hat{A} = NA_k M^T + NB_k CX + YBC_k M^T + YA_N X$, $\hat{B} = NB_k$, $\hat{C} = C_k M^T$, $\eta = \gamma^2$ and selecting $\delta = 1$, we obtain

$$\Omega_5 + \Gamma_{12} \Gamma_{22}^{-1} \Gamma_{12}^T \prec 0$$

where

$$\Omega_5 = \begin{bmatrix} \Omega_{11} & \Omega_{12} & \Omega_{13} & \Omega_{14} \\ \Omega_{21} & \Omega_{22} & \Omega_{23} & \Omega_{24} \\ \Omega_{31} & \Omega_{32} & \Omega_{33} & \Omega_{34} \\ \Omega_{41} & \Omega_{42} & \Omega_{43} & \Omega_{44} \end{bmatrix},$$

with

$$\begin{aligned}\Omega_{11} &= A_N X + X A_N^T + B \hat{C} + \hat{C}^T B^T + (\epsilon_1 + \epsilon_2) L L^T, \\ \Omega_{12} &= \Omega_{21}^T = \hat{A}^T + A_N \\ \Omega_{22} &= A_N^T Y + Y A_N + \hat{B} C + C^T \hat{B}^T + \epsilon_3 R^T R, \\ \Omega_{13} &= \Omega_{31}^T = B_d, \quad \Omega_{14} = \Omega_{41}^T = X C_z^T + \hat{C}^T D_z^T, \\ \Omega_{23} &= \Omega_{32}^T = Y B_d, \quad \Omega_{24} = \Omega_{42}^T = C_z^T, \quad \Omega_{33} = -\eta I, \\ \Omega_{34} &= \Omega_{43} = 0, \quad \Omega_{44} = -I.\end{aligned}$$

Moreover, we have

$$\begin{aligned}\Gamma_{12} &= \begin{bmatrix} XR^T & 0 & 0 & YL & 0 \\ 0 & R^T & YL & 0 & XR^T \\ 0 & 0 & 0 & 0 & 0 \\ 0 & 0 & 0 & 0 & 0 \end{bmatrix}, \\ \Gamma_{22} &= -\text{diag}(\epsilon_1 I, \epsilon_2 I, \epsilon_3 I, I, I).\end{aligned}$$

Finally, by applying Lemma 3, the LMIs in (33) are obtained.

ACKNOWLEDGEMENT

This work was supported in part by the Swiss National Science Foundation (SNSF) under the project RECCE, ‘‘Real-time traffic estimation and control in a connected environment’’, contract No. 200021-188622.

REFERENCES

- [1] Y. A. Harfouch, S. Yuan, and S. Baldi, ‘‘An adaptive switched control approach to heterogeneous platooning with intervehicle communication losses,’’ *IEEE Trans. Contr. Netw. Syst.*, vol. 5, no. 3, pp. 1434–1444, 2017.
- [2] V. Giammarino, M. Lv, S. Baldi, P. Frasca, and M. L. Delle Monache, ‘‘On a weaker notion of ring stability for mixed traffic with human-driven and autonomous vehicles,’’ in *Proc. 58th IEEE Conf. on Decision and Control*, 2019, pp. 335–340.
- [3] I. Papamichail, K. Kampitaki, M. Papageorgiou, and A. Messmer, ‘‘Integrated ramp metering and variable speed limit control of motorway traffic flow,’’ *IFAC Proc. Vol.*, vol. 41, no. 2, pp. 14 084–14 089, 2008.
- [4] G. J. Naus, R. P. Vugts, J. Ploeg, M. J. van De Molengraft, and M. Steinbuch, ‘‘String-stable cacc design and experimental validation: A frequency-domain approach,’’ *IEEE Trans. Vehicular Tech.*, vol. 59, no. 9, pp. 4268–4279, 2010.
- [5] V. Milanés, S. E. Shladover, J. Spring, C. Nowakowski, H. Kawazoe, and M. Nakamura, ‘‘Cooperative adaptive cruise control in real traffic situations,’’ *IEEE Trans. Intell. Transport. Syst.*, vol. 15, no. 1, pp. 296–305, 2013.
- [6] A. Alam, J. Mårtensson, and K. H. Johansson, ‘‘Experimental evaluation of decentralized cooperative cruise control for heavy-duty vehicle platooning,’’ *Contr. Engin. Pract.*, vol. 38, pp. 11–25, 2015.
- [7] S. E. Li, Y. Zheng, K. Li, Y. Wu, J. K. Hedrick, F. Gao, and H. Zhang, ‘‘Dynamical modeling and distributed control of connected and automated vehicles: Challenges and opportunities,’’ *IEEE Intell. Transport. Syst. Mag.*, vol. 9, no. 3, pp. 46–58, 2017.
- [8] Y. Sugiyama, M. Fukui, M. Kikuchi, K. Hasebe, A. Nakayama, K. Nishinari, S.-i. Tadaki, and S. Yukawa, ‘‘Traffic jams without bottlenecks—experimental evidence for the physical mechanism of the formation of a jam,’’ *New J. Phys.*, vol. 10, no. 3, p. 033001, 2008.
- [9] M. R. Flynn, A. R. Kasimov, J.-C. Nave, R. R. Rosales, and B. Seibold, ‘‘Self-sustained nonlinear waves in traffic flow,’’ *Phys. Rev. E*, vol. 79, no. 5, p. 056113, 2009.
- [10] K. Nagel and M. Schreckenberg, ‘‘A cellular automaton model for freeway traffic,’’ *J. Phys. I France*, vol. 2, no. 12, pp. 2221–2229, 1992.
- [11] M. Bando, K. Hasebe, A. Nakayama, A. Shibata, and Y. Sugiyama, ‘‘Dynamical model of traffic congestion and numerical simulation,’’ *Phys. Rev. E*, vol. 51, no. 2, p. 1035, 1995.
- [12] R. E. Stern, S. Cui, M. L. Delle Monache, R. Bhadani, M. Bunting, M. Churchill, N. Hamilton, H. Pohlmann, F. Wu, B. Piccoli, *et al.*, ‘‘Dissipation of stop-and-go waves via control of autonomous vehicles: Field experiments,’’ *Transp. Res. Part C: Emerging Tech.*, vol. 89, pp. 205–221, 2018.
- [13] S. Cui, B. Seibold, R. Stern, and D. B. Work, ‘‘Stabilizing traffic flow via a single autonomous vehicle: Possibilities and limitations,’’ in *IEEE Intell. Vehicles Sympos.*, 2017, pp. 1336–1341.
- [14] D. Swaroop and J. K. Hedrick, ‘‘String stability of interconnected systems,’’ *IEEE Trans. Automat. Contr.*, vol. 41, no. 3, pp. 349–357, 1996.
- [15] J. Ploeg, N. Van De Wouw, and H. Nijmeijer, ‘‘Lp string stability of cascaded systems: Application to vehicle platooning,’’ *IEEE Trans. Contr. Syst. Tech.*, vol. 22, no. 2, pp. 786–793, 2013.
- [16] V. Giammarino, S. Baldi, P. Frasca, and M. L. Delle Monache, ‘‘Traffic flow on a ring with a single autonomous vehicle: An interconnected stability perspective,’’ *IEEE Trans. Intell. Transport. Syst.*, 2020.
- [17] A. Talebpour and H. S. Mahmassani, ‘‘Influence of connected and autonomous vehicles on traffic flow stability and throughput,’’ *Transp. Res. Part C: Emerg. Tech.*, vol. 71, pp. 143–163, 2016.
- [18] D.-F. Xie, X.-M. Zhao, and Z. He, ‘‘Heterogeneous traffic mixing regular and connected vehicles: Modeling and stabilization,’’ *IEEE Trans. Intell. Transport. Syst.*, vol. 20, no. 6, pp. 2060–2071, 2018.
- [19] M. Treiber, A. Hennecke, and D. Helbing, ‘‘Congested traffic states in empirical observations and microscopic simulations,’’ *Phys. rev. E*, vol. 62, no. 2, p. 1805, 2000.
- [20] C. Wu, A. M. Bayen, and A. Mehta, ‘‘Stabilizing traffic with autonomous vehicles,’’ in *IEEE Int. Conf. Robot. Autom. (ICRA)*, 2018, pp. 6012–6018.
- [21] M. L. Delle Monache, T. Liard, A. Rat, R. Stern, R. Bhadani, B. Seibold, J. Sprinkle, D. B. Work, and B. Piccoli, ‘‘Feedback control algorithms for the dissipation of traffic waves with autonomous vehicles,’’ in *Computational Intelligence and Optimization Methods for Control Engineering*, 2019, pp. 275–299.
- [22] Y. Zheng, J. Wang, and K. Li, ‘‘Smoothing traffic flow via control of autonomous vehicles,’’ *IEEE Internet of Things J.*, 2020.

- [23] J. Wang, Y. Zheng, Q. Xu, J. Wang, and K. Li, "Controllability analysis and optimal control of mixed traffic flow with human-driven and autonomous vehicles," *IEEE Trans. Intell. Transport. Syst.*, 2020.
- [24] Mousavi, Shima Sadat and Haeri, Mohammad and Mesbahi, Mehran, "On the structural and strong structural controllability of undirected networks," *IEEE Trans. Automat. Contr.*, vol. 63, no. 7, pp. 2234–2241, 2018.
- [25] S. S. Mousavi, M. Haeri, and M. Mesbahi, "Strong structural controllability of networks under time-invariant and time-varying topological perturbations," *IEEE Trans. Automat. Contr.*, vol. 66, no. 3, pp. 1375–1382, 2021.
- [26] —, "Laplacian dynamics on cographs: Controllability analysis through joins and unions," *IEEE Trans. Automat. Contr.*, vol. 66, no. 3, pp. 1383–1390, 2021.
- [27] F. M. Callier and C. A. Desoer, *Linear system theory*. New York, NY, USA: Springer Science & Business Media, 2012.
- [28] J. Wang, Y. Zheng, Q. Xu, J. Wang, and K. Li, "Controllability analysis and optimal controller synthesis of mixed traffic systems," in *IEEE Intell. Vehicles Sympos.*, 2019, pp. 1041–1047.
- [29] C. Chen, J. Wang, Q. Xu, J. Wang, and K. Li, "Mixed platoon control of automated and human-driven vehicles at a signalized intersection: dynamical analysis and optimal control," *Transport. Res. Part C: Emerg. Technol.*, vol. 127, p. 103138, 2021.
- [30] J. Wang, Y. Zheng, C. Chen, Q. Xu, and K. Li, "Leading cruise control in mixed traffic flow: System modeling, controllability, and string stability," *arXiv:2012.04313*, 2020.
- [31] I. G. Jin and G. Orosz, "Optimal control of connected vehicle systems with communication delay and driver reaction time," *IEEE Trans. Intell. Transport. Syst.*, vol. 18, no. 8, pp. 2056–2070, 2016.
- [32] C. Wu, A. Kreidieh, E. Vinitzky, and A. M. Bayen, "Emergent behaviors in mixed-autonomy traffic," in *Conference on Robot Learning*, 2017, pp. 398–407.
- [33] S. Gong and L. Du, "Cooperative platoon control for a mixed traffic flow including human drive vehicles and connected and autonomous vehicles," *Transport. Res. Part B: Method.*, vol. 116, pp. 25–61, 2018.
- [34] A. R. Kreidieh, C. Wu, and A. M. Bayen, "Dissipating stop-and-go waves in closed and open networks via deep reinforcement learning," in *21st Internat. Conf. Intell. Transport. Syst.*, 2018, pp. 1475–1480.
- [35] M. Di Vaio, G. Fiengo, A. Petrillo, A. Salvi, S. Santini, and M. Tufo, "Cooperative shock waves mitigation in mixed traffic flow environment," *IEEE Trans. Intell. Transport. Syst.*, vol. 20, no. 12, pp. 4339–4353, 2019.
- [36] E. Vinitzky, K. Parvate, A. Kreidieh, C. Wu, and A. Bayen, "Lagrangian control through deep-rl: Applications to bottleneck decongestion," in *21st Internat. Conf. Intell. Transport. Syst.*, 2018, pp. 759–765.
- [37] J. Monteil, M. Bouroche, and D. J. Leith, " \mathcal{L}_2 and \mathcal{L}_∞ stability analysis of heterogeneous traffic with application to parameter optimization for the control of automated vehicles," *IEEE Trans. Contr. Syst. Tech.*, vol. 27, no. 3, pp. 934–949, 2018.
- [38] M. R. Jovanović and N. K. Dhingra, "Controller architectures: Tradeoffs between performance and structure," *Europ. J. Contr.*, vol. 30, pp. 76–91, 2016.
- [39] I. G. Jin, S. S. Avedisov, C. R. He, W. B. Qin, M. Sadeghpour, and G. Orosz, "Experimental validation of connected automated vehicle design among human-driven vehicles," *Transport. Res. Part C: Emerg. Technol.*, vol. 91, pp. 335–352, 2018.
- [40] N. Chen, M. Wang, T. Alkim, and B. van Arem, "A robust longitudinal control strategy of platoons under model uncertainties and time delays," *J. Advanced Transport.*, vol. 2018, 2018.
- [41] S. Feng, Z. Song, Z. Li, Y. Zhang, and L. Li, "Robust platoon control in mixed traffic flow based on tube model predictive control," *IEEE Trans. on Intell. Vehicles*, 2021.
- [42] G. Orosz, "Connected cruise control: modelling, delay effects, and nonlinear behaviour," *Veh. Syst. Dyn.*, vol. 54, no. 8, pp. 1147–1176, 2016.
- [43] R. A. Horn and C. R. Johnson, *Matrix Analysis*. Cambridge University Press, 2012.
- [44] E. D. Sontag, *Mathematical Control Theory: Deterministic Finite Dimensional Systems*. New York: Springer Verlag, 1998.
- [45] C. Scherer, P. Gahinet, and M. Chilali, "Multiobjective output-feedback control via lmi optimization," *IEEE Trans. Automat. Contr.*, vol. 42, no. 7, pp. 896–911, 1997.
- [46] S. Boyd, L. El Ghaoui, E. Feron, and V. Balakrishnan, *Linear Matrix Inequalities in System and Control Theory*. Philadelphia, PA: Siam, 1994, vol. 15.
- [47] Y. Wang, L. Xie, and C. E. De Souza, "Robust control of a class of uncertain nonlinear systems," *Systems & control letters*, vol. 19, no. 2, pp. 139–149, 1992.
- [48] F. Zhang, *The Schur Complement and its Applications*. Springer Science & Business Media, 2006, vol. 4.